

## Power Quality Enhancement in Distribution System Using Shunt Active Power Filter with ANFIS Controller

**K. Suvarana**

PG Student,  
[kanikitisuvarana@gmail.com](mailto:kanikitisuvarana@gmail.com),  
 Department of EEE,  
 SKU College of Engg.and Tech.,  
 SK University, Anantapuramu-515 003.

**V. K. Chakravarthi Naik**

Lecturer,  
[Coolchakri97@gmail.com](mailto:Coolchakri97@gmail.com),  
 Department of EEE,  
 SKU College of Engg.and Tech.,  
 SK University, Anantapuramu-515 003.

**Abstract:-** *An active power filter integrated with a four-leg voltage-source inverter by means of a predictive control method is mentioned. This paper will provide a novel control technique for utilizing optimal benefits from the power grid interfacing inverters, when installed in 3-phase 4-leg distribution system. An extensive but basic mathematical model of the active power filter, which includes the impact of the equivalent power system impedance, is obtained and even useful to layout the predictive control algorithm. The inverter is controlled to perform as multi-function system by including shunt active power filter (SAPF) features. The harmonic current compensation procedure will depend on current reference generation, a technique distinctive from regular techniques, which involve signals of harmonics and reactive power components of the load. The control strategy carried out is by using PI, ANFIS controllers together with hysteresis control. This control scheme possesses the advantage of good stability and strong regulation capability. The test is practiced in the MATLAB/SIMULINK. Distinct simulation results are displayed under steady state and transient operating conditions and the overall performance of ANFIS and PI controllers is compared.*

**Keywords:-** *Shunt Active power filters (SAPF), four-leg voltage source inverter, predictive control, Hysteresis current control, adaptive neuro fuzzy inference system (ANFIS)controller, Total Harmonic Distortion (THD).*

### I INTRODUCTION

Renewable energy sources also called non-conventional energy sources that are continuously replenished by natural processes [1]. For an example, photo voltaic power, wind power, bio-energy - bio-fuels developed sustainably, hydropower and many more., are some of the examples of renewable sources A renewable energy system are able to

convert the energy within sunlight, wind, falling water, sea-waves, geothermal heat, or biomass into an application, we can use such as heat or electricity. Majority of the renewable energy is available either instantly or in certain way from sun and wind and can never be exhausted, thereby these are termed renewable.

In modern electrical distribution systems there has been a sudden increase of single phase and three-phase non-linear loads [2]-[6]. Such non-linear loads make use of solid state power conversions and extract non-sinusoidal currents from AC mains and cause harmonics and reactive power burden, and a severe neutral current that causes polluting of power systems. In addition they result in lower efficiency and interruption to nearby communication networks and other equipments.

Active power filters has been developed to eliminate such kind of issues. Shunt active filters based upon current controlled PWM converters are viewed as promising approach. The methods that are used to produce preferred compensating current are based upon instantaneous extraction of compensating commands from the distorted currents or voltage signals in time domain.

Electric utilities and end users of electric power are becoming increasingly concerned about meeting the growing energy demand [7]-[8]. Seventy-five percentage of entire global energy demand is available by the heating of fossil fuels.

Renewable energy source (RES) integrated at distribution level is termed as distributed generation (DG) [9]. The electric resource is conscious because of the great penetration level of

unpredictable RES in distribution systems since it could create a hazard to network regarding stability, voltage regulation and power-quality (PQ) concerns. diminish the quality of power. In general, current controlled voltage source inverters are employed interface the intermittent RES in distributed system. Active power filters (APF) are widely familiar to counteract the load current harmonics and load

On the other hand, the widespread use of power electronics based devices and non-linear loads at PCC produce harmonic currents, which can easily unbalance at distribution level. Power Quality is simply defined as the physical characteristics of the electrical supply provided under normal operating conditions which will not interrupt the customer's practice.

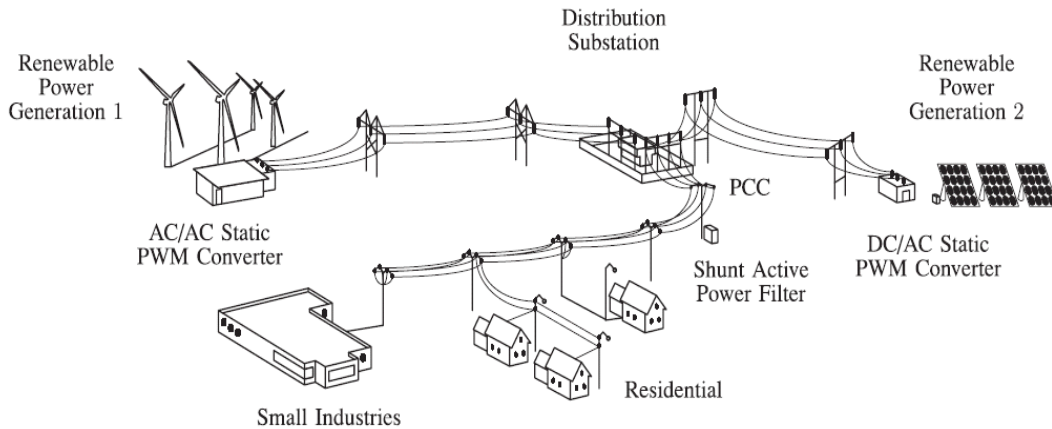


Fig.1. Stand-alone shunt active power filter for hybrid power generation system.

**II THREE-PHASE FOUR-LEG CONVERTER MODEL**

Fig.1 represents the configuration of atypical power distribution system with renewable power generation. It consists of various types or power generation units and different types of loads. Renewable sources, such as wind and sunlight, are typically used to generate electricity for residential users and small industries. Both types of power generation use ac/dc and dc/ac static PWM converters for battery banks and voltageconversion for long-term energy storage [3]-[4]. As the electrical energy consumption behavior is random and unpredictable, and therefore, it may be three-phase or single-phase, un-balanced or balanced, and non-linear or linear. A shunt active power filter is coupled in parallel at the point of common coupling to compensate current harmonics, current balance, and reactive power. It is composed by electrolytic capacitor, a four-leg PWM converter, and a first-order output ripple filter, as shown in fig. 2.

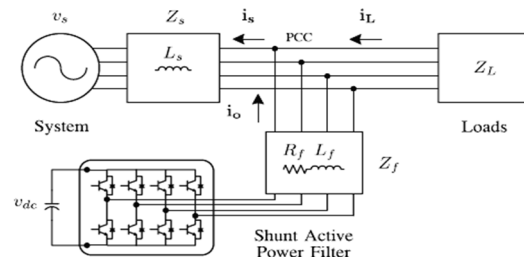


Fig. 2. Equivalent model of Three-phase shunt active power filter.

This circuit considers the equivalent power system impedance  $Z_s$ , the converter output ripple filter impedance  $Z_f$ , and load impedance  $Z_L$ . The three-phase four-leg PWM converter topology is as shown in fig. 3. This converter topology is analogous to the conventional three-phase converter with the fourth leg connected to the neutral bus of the system. The fourth leg increases switching states from  $8(2^3)$  to  $16(2^4)$ , improving control flexibility and output voltage quality [4], and suitable for current unbalanced compensation.

The switching prototype of each IGBT inside inverter can be formulate on the basis of error between real and reference current of inverter, which can be explained as:

If  $I_{inv,a} < I_{inv,a}^* - hb$  then upper switch S1 will be OFF and lower switch S2 will be ON in the phase-a leg of inverter.

If  $I_{inv,a} > I_{inv,a}^* + hb$  then upper switch S1 will be ON and lower switch S2 will be OFF in the phase-a leg inverter. Where hb is the width hysteresis band (hb). On the similar principle, the switching pulses for remaining otherthree legs can be derived.

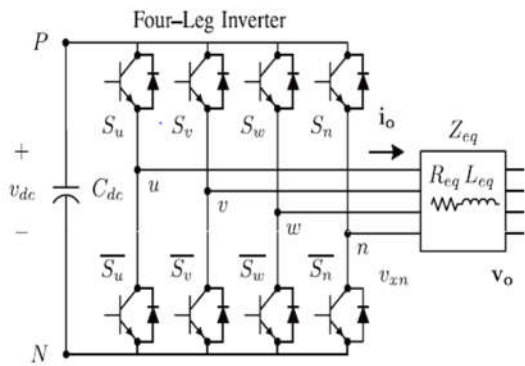


Fig. 3. Two-level four-leg PWM-VSI topology.

The voltage in whichever leg x of the converter, calculated from the neutral point(n), and can be uttered in terms of switching states, as below,

$$V_{xn} = (S_x - S_n)V_{dc}, \quad x=u,v, w, n \quad (1)$$

The mathematical representation of the filter derived from the corresponding circuit shown in fig. 2 is

$$V_0 = V_{xn} - R_{eq}i_0 - L_{eq} \frac{di_0}{dt} \quad (2)$$

Where  $R_{eq}$  and  $L_{eq}$  are the 4L-VSI output parameters expressed as Thevenin impedances at the converter output terminals  $Z_{eq}$ . Therefore, the thevenin equivalent impedance is determined by a series connection of the ripple filter impedance  $Z_f$  and a parallel arrangement between the system equivalent impedance  $Z_s$  and the load impedance  $Z_L$ .

$$Z_{eq} = \frac{Z_s Z_L}{Z_s + Z_L} + Z_f \approx Z_s + Z_f \quad (3)$$

For this model, it is assumed that  $Z_L \gg Z_s$ , and the resistive element of the system's equivalent impedance is ignored, and that the series reactance is in the range of 3-7% p.u., which is a satisfactory approximation of the actual system. at last, in equation(2)

$$R_{eq} = R_f \text{ and } L_{eq} = L_s + L_f$$

### III PREDICTIVE CURRENT CONTROL

A system model is employed to estimate the current values of the output parameters. The residuals, the changes between the actual and predicted outputs, function as the feedback signal to a Prediction block. The predictions are widely-used in two forms of predictive analysis which are carried out at every sampling instant: set-point calculations and control calculations. The block diagram of the suggested predictive current control scheme is shown in Fig. 4.

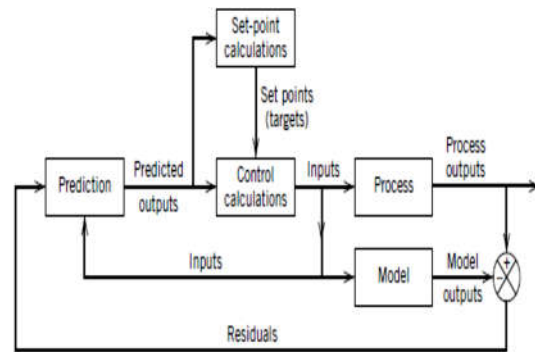


Fig.4. Block diagram of the predictive control scheme.

Inequality constraints on the input and output variables, such as upper and lower limits, can be included in either type of calculation. Note that the predictive configuration is similar to both the internal model control configuration in and the Smith predictor configuration, because the model acts in parallel with the process and the residual serves as a feedback signal. Still, the co-ordination of the control and set-point calculations is a distinct aspect of predictive control.

### A .Source reference current generator

The max value of the reference current  $I_{sp}$  can be calculated by controlling the DC side capacitor voltage. Ultimate compensation needs the mains current to be sinusoidal and in phase with the source voltage, irrespective of the load current [6] the desired source currents, after compensation, can be given as

$$\begin{aligned}(I_{SU}^*) &= I_{SP} \sin \omega t \\ (I_{SV}^*) &= I_{SP} \sin(\omega t - 90) \\ (I_{SW}^*) &= I_{SP} \sin(\omega t + 90) \\ (I_{SN}^*) &= I_{SP} \sin \omega t \quad (3)\end{aligned}$$

Where  $I_{sp} (=I_1 \cos \phi_1 + I_{s1})$  the amplitude of the desired source current, the while the phase angle can be obtained from the source voltages. Hence, the waveform and phases of the source currents are known, and only the magnitudes of the source currents need to be determined. This peak value of the reference current has been estimated by regulating the DC side capacitor voltage of the PWM converter. This capacitor voltage is compared with the reference value and the error is processed in fuzzy controller. The output of the fuzzy controller has been considered as the amplitude of the desired source current, and the reference currents are estimated by multiplying this peak value with unit sine vectors in phase with the source voltages.

### B. Predictive model

The converter model is used to predict the output converter current. Since the controller operates in discrete time, both the controller and the system model must be represented in a discrete time domain. The discrete time model consists of a recursive matrix equation that represents this prediction system. This means that for a given sampling time  $T_s$ , knowing the converter switching states and control variables at instant  $kT_s$ , it is possible to predict the next states at any instant  $[k + 1]T_s$ .

Due to the first-order characteristics of the condition equations that portray the model from equations 1 and 2, a adequately genuine first-order estimation of the derivative is considered in this paper.

$$\frac{dx}{dt} \approx \frac{x[k+1]-x[k]}{t_s} \quad (4)$$

The 16 possible output current predicted values can be obtained from (2) and (4) as

$$i_0[k + 1] = \frac{t_s}{L_{eq}} (V_{xn}[k] - V_0[k]) + \left(1 - \frac{r_{eq} t_s}{L_{eq}}\right) i_0[k] \quad (5)$$

As shown in (5), with a view to predict the output current  $i_0$  at the instant  $(k + 1)$ , the input voltage value  $v_0$  and the converter output voltage  $V_{xn}$ , are essential. The algorithm determines entirely 16 values related to the possible combinations that the state parameters can attain.

### C. Cost function optimization

In order to select the optimal switching state that must be applied to the power converter, the 16 predicted values obtained for  $i_0[k + 1]$  are in contrast to the reference using a cost function  $g$ , provided below,

$$\begin{aligned}g[k+1] &= [i_{ou}^*[k + 1] - i_{ou}[k + 1]]^2 \\ &+ [i_{ov}^*[k + 1] - i_{ov}[k + 1]]^2 \\ &+ [i_{ow}^*[k + 1] - i_{ow}[k + 1]]^2 \\ &+ [i_{on}^*[k + 1] - i_{on}[k + 1]]^2. \quad (6)\end{aligned}$$

The output current ( $i_0$ ) is similar to the reference when  $g =$  zero. Consequently, the optimization target of the cost function is to achieve a  $g$  value near to zero. The voltage vector (from 2) that reduces the cost function is selected then simply implemented at the subsequent sampling state. In each sampling state, the switching state that generates the minimum value of  $g$  is selected from the 16 possible function values. The algorithm selects the switching state that produces this minimum value and applies it to the converter during the  $k + 1$  state.

#### IV CURRENT REFERENCE GENERATION

The control circuit of a SAPF performs three functions:

1. Reference current generation-analyze the current reference wave form for every phase of the inverter.
2. DC link voltage control-uphold the constant voltage of DC link capacitor.
3. Gating signal generation-produce the inverter gating signals.

There are several possibilities to find out the reference current necessary for compensating the non-linear loads. In general, shunt active power filters are used to compensate the displacement power factor and low-frequency current harmonics generated by non-linear loads. In this paper instantaneous reactive power (IRP) theory is used for reference current generation.

The displacement power factor  $\sin \phi_{(L)}$  and the maximum total harmonic distortion of the load  $THD_{(L)}$  shows the relationship between the apparent power necessary by the active power filter, with respect to the load, as shown

$$\frac{S_{SAPF}}{S_L} = \frac{\sqrt{\sin \phi_{(L)} + THD_{(L)}^2}}{\sqrt{1 + THD_{(L)}^2}} \quad (7)$$

The  $\sin(\omega t)$  and  $\cos(\omega t)$  synchronized reference signals are obtained from a synchronous reference frame (SRF) PLL [8]. The SRF-PLL generates a pure sinusoidal wave form even when the system voltage is severely distorted. Tracking errors are eliminated, since SRF-PLLs are designed to avoid phase voltage unbalancing, harmonics (i.e., less than 5% and 3% in fifth and seventh, respectively), and offset caused by the nonlinear load conditions and measurement errors [30]. Equation (8) shows relationship between the real currents  $i_{Lx(t)}$  (x=u, v, w) and the related dq components (id and iq)

$$\begin{bmatrix} i_d \\ i_q \end{bmatrix} = \sqrt{\frac{2}{3}} \begin{bmatrix} \sin \omega t & \cos \omega t \\ -\cos \omega t & \sin \omega t \end{bmatrix} \times \begin{bmatrix} 1 & -\frac{1}{2} & -\frac{1}{2} \\ 0 & \frac{\sqrt{3}}{2} & -\frac{\sqrt{3}}{2} \end{bmatrix} \quad (8)$$

A low-pass filter (LPF) extracts the dc component of the phase currents id to generate the harmonic reference components  $i_d^*$  and  $i_q^*$ . The reactive components of the phase-currents are obtained by phase shifting the corresponding ac and

dc components of iq by 180 degrees. Consecutively to maintain the dc-voltage constant, the amplitude of the converter reference current must be customized by adding an active power reference signal i.e. with the component, as explained. The resultant signals  $i_d^*$  and  $i_q^*$  are transformed back to a three-phase system by applying the inverse park and Clark transformation, as shown in (9). The cut-off frequency of the LPF used in this paper is 4.63 KHz.

$$\begin{bmatrix} i_{0u}^* \\ i_{0v}^* \\ i_{0w}^* \end{bmatrix} = \sqrt{\frac{2}{3}} \begin{bmatrix} \frac{1}{\sqrt{2}} & 1 & 0 \\ \frac{1}{\sqrt{2}} & -\frac{1}{2} & \frac{\sqrt{3}}{2} \\ \frac{1}{\sqrt{2}} & -\frac{1}{2} & -\frac{\sqrt{3}}{2} \end{bmatrix} \times \begin{bmatrix} 1 & 0 & 0 \\ 0 & \sin \omega t & -\cos \omega t \\ 0 & \cos \omega t & \sin \omega t \end{bmatrix} \begin{bmatrix} i_d^* \\ i_q^* \end{bmatrix} \quad (9)$$

The current that flows throughout the neutral of the load is compensated by injecting the same instantaneous value obtained from the phase-currents, phase-shifted by 180 degrees, as shown below

$$i_{0n}^* = -(i_{Lu} + i_{Lv} + i_{Lw}) \quad (10)$$

One of the foremost advantages of the dq-base current reference generator method is that it allows execution of linear controller in dc-voltage control loop. However, one important disadvantage of the dq-based current reference frame algorithm used to generate the current reference is that a second order harmonic component is generated in id and iq under unbalanced operating conditions. The amplitude of this harmonic depends on the percent of unbalanced load current (expressed as the relationship between the negative sequence current  $i_L$ , and the positive sequence current  $i_L$ ).

The second-order harmonic cannot be removed from  $i_d$  and  $i_q$  and consequently generates at third harmonic in the reference current when it is converted back to abc frame [9]-[10]. The load current does not contain a third harmonic, the one generated by the active power filter to the power system.

#### V HYSTERESIS CURRENT CONTROLLER

The current controller selects the switching patterns of the devices in the SAPF. The switching logic is formulated as,

If  $(i_{sa} < i_{sa}^* - hb)$  lower switch is ON and upper switch is OFF in leg “a” of the SAPF;

If  $(i_{sa} > i_{sa}^* - hb)$  lower switch is OFF and upper switch is ON in leg “a” of the SAPF.

Correspondingly, the switches in the legs “b” and “c” are done. Here, hb is the width of the hysteresis band of the reference currents. In this manner, the supply currents are regulated within the hysteresis band of their respective reference values. The performance of active filter is analyzed by solving set of differential equations, with further expressions.

**A. PI controller**

PI controllers have two tuning parameters to regulate. While this makes them more demanding to tune than a PI controller, they are not as difficult as the three parameter PID controller [8]. Integral action enables PI controllers to eliminate offset, a major weakness of a p-only controller. Thus, PI controllers provide a balance of complexity and capability that makes by distant. The most widely used algorithm in process control applications proportional plus integral (PI) were developed because of the desirable property in that system with open loop transfer functions of type1 or above have zero steady state error with respect to a step input. The PI regulator general equation the input E(s) and output U(s) is given as,

$$\frac{U(s)}{E(s)} = k_p + \frac{k_i}{s} \tag{11}$$

**B. ANFIS controller**

Adaptive fuzzy neuro inference system (ANFIS) is a hybrid advance to deal the linguistic variables and numerical variable. Fig.7 shows general diagram of ANFIS controller. In fuzzy the linguistic variables by system behavior in ANN are chosen and are used to tune the membership function. Sugeno type function is utilized to design ANFIS due to its output is always linear or constant [9]-[10]. The output of each rule  $Z_i$  is firing strength of the  $W_i$  of each rule. And rule aforementioned here is firing strength is given by  $W_i = \text{AND} [F_1(x), F_2(x)]$  where F(.) is the inputs of the 1 and 2.

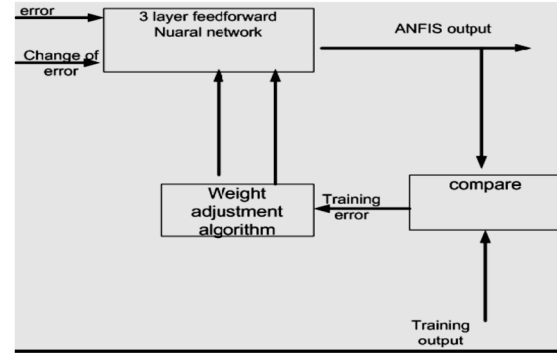


Fig.5. ANFIS control for APF.

**C. Design of Adaptive Neuro-Fuzzy controller**

Adaptive neuro fuzzy inference system (ANFIS) integrates the finest features of fuzzy systems and neural networks, and it has prospective to capture the benefits of both in a single frame work [9]. ANFIS is a kind of artificial neural network that is based on Takagi-sugeno fuzzy inference system, which is having one input and one output. Using a given data set, the toolbox function of ANFIS constructs a fuzzy inference system (FIS) where as the membership function parameters are tuned (adjusted) using a back propagation algorithm. In order to have an idea of optimized ANFIS architecture for proposed control, an initial data is generated from normal PI regulator and the data is saved in workspace of MATLAB. Then the data previously saved in workspace is located in the ANFIS command window to generate an optimized ANFIS architecture as shown fig.6.

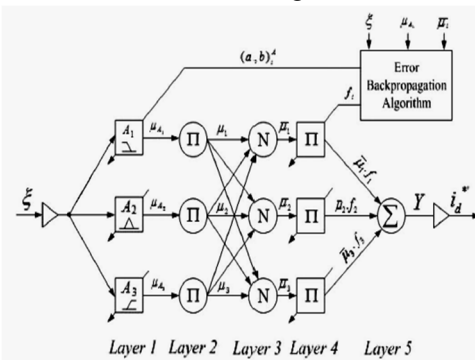


Fig.6. Schematic of the proposed ANFIS-based control architecture.

The node functions of each layer in the ANFIS architecture are described as follows :

The error between reference dc-link voltage and actual dc-link voltage ( $e = v_{dc}^* - V_{dc}$ ) is given to the neuro-fuzzy controller and the same error is used to tune the precondition and Consequent parameters [11]. The control of dc-link voltage gives the active power current component ( $i_d^*$ ), which is further customized to take in account of active current component injected from RES ( $i_{RES}$ ). The node functions of each and every layer in ANFIS architecture are as described below:

Layer 1: This layer is also recognized as fuzzification layer where each node is represented by square. Here, three membership functions are assigned to each input. The trapezoidal and triangular membership functions are used to reduce the computation burden as shown in fig. 10, and corresponding node equations are as given below

$$U_{A1}(\varepsilon) = \begin{cases} 1 & \varepsilon \leq b_1 \\ \frac{\varepsilon - a_1}{b_1 - a_1} & b_1 < \varepsilon < a_1 \\ 0 & \varepsilon \geq a_1 \end{cases} \quad (12)$$

$$U_{A2}(\varepsilon) = \begin{cases} 1 - \frac{\varepsilon - a_1}{0.5b_2} & |\varepsilon - a_2| \leq 0.5b_2 \\ 0 & |\varepsilon - a_2| > 0.5b_2 \end{cases} \quad (13)$$

$$U_{A3}(\varepsilon) = \begin{cases} 0 & \varepsilon \leq a_3 \\ \frac{\varepsilon - a_1}{b_1 - a_1} & a_3 < \varepsilon < b_3 \\ 1 & \varepsilon \geq b_3 \end{cases} \quad (14)$$

Where the value of parameters ( $a_i, b_i$ ) changes with the change in error and hence generates the linguistic value of each membership function. Parameters in this layer are referred as premise parameters or precondition parameters.

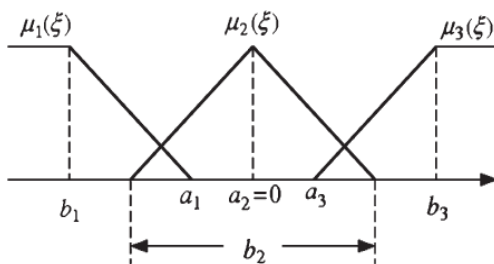


Fig.7. Fuzzy membership functions.

Layer 2: Every node in this layer is a circle named as  $\pi$ , which multiplies the incoming signals and extends it to next layer.

$$U_i = U_{Ai}(\varepsilon_1) \cdot U_{Bi}(\varepsilon_2) \dots \dots \dots i = 1, 2, 3. \quad (15)$$

But in this case there is only one input, so this layer can be ignored and the output of first layer will directly forwarded to the third layer. Here, the output of each node represents the firing strength of a rule.

Layer 3: Every node in this layer is represented as circle. This layer calculates the normalized firing strength of each rule as given below:

$$\bar{\alpha}_i = \frac{\alpha_i}{\alpha_1 + \alpha_2 + \alpha_3} \quad (16)$$

Layer 4: Every node in this layer is a node function

$$O_i = \bar{\alpha}_i f_i(a_0^i + a_1^i \varepsilon) \quad (17)$$

$$i = 1, 2, 3, \dots$$

Where the parameters ( $a_0^i, a_1^i$ ) are tuned as the function of input ( $\xi$ ). The parameters in this layer are also referred as consequent parameters.

Layer 5: This layer is also called output layer which computes the output as given below:

$$Y = \bar{\alpha}_1 f_1 + \bar{\alpha}_2 f_2 + \bar{\alpha}_3 f_3 \quad (18)$$

The output from this layer is then multiplied with the normalizing factor to obtain the active power current component ( $i_d^*$ ).

## VI DC LINK VOLTAGE CONTROL

In addition with the fundamental current section of load current, the source should also supply another fundamental current component to continue DC link capacitor voltage to a preferred constant value. This second component of source current is necessary to supply the losses in the converter such as ohmic loss, switching losses; capacitor voltage loss etc. voltage across DC link capacitor  $V_{dc}$  can be used to detect losses in the system. If,  $V_{dc,ref}$  - Reference voltage of DC link capacitor,

$V_{dc}$  - Actual voltage of DC link capacitor,  
Then, error signal  $e = V_{dc,ref} - V_{dc}$ .

This signal error is given to PI controller, output of which a current template is and is multiplied with  $V_{dc,ref}$  to obtain the loss component  $P_{loss}$  [12]. From the above equations reference SAPF

current can be calculated which are assigned to the hysteresis current controller (HCC) to produce the switching signals of the inverter. In this fashion PI controller is utilized to maintain the stable DC link capacitor voltage as shown in figure (8).

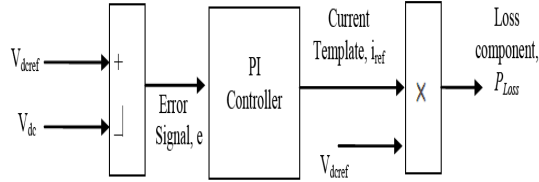


Fig.8. PI controller used for DC link capacitor voltage balancing.

The dc-voltage remains stable (with a minimum value of  $\sqrt{6}V_s$  (rms)) until the active power absorbed by the converter decreases to a level where it is not capable to compensate for its losses. The active power absorbed by the converter is controlled by regulating the amplitude of the active power reference signal, which is in-phase with each phase voltage. The block diagram shown in fig. 8, the dc-voltage  $V_{dc}$  is measured and then compared with a constant reference value  $V_{dc}^*$ . The error (e) is processed by a PI controller, with two gains,  $K_p$  and  $K_i$ . Both gains are calculated according to the dynamic response condition. Fig. 8 shows that the output of the controller is fed to the dc-voltage transfer function  $G(s)$ , which is represented by a first-order system (19),

$$G(s) = \frac{v_{dc}}{i_e} = \frac{3}{2} \frac{k_p V_s}{c_{dc} V_{dc}^*} \quad (19)$$

The equivalent closed-loop transfer function of the given system with a PI controller (20) is shown in (21).

$$C(s) = k_p + \left(1 + \frac{1}{T_{i,s}}\right) \quad (20)$$

$$\frac{v_{dc}}{i_e} = \frac{\omega_n^2 (s+a)}{s^2 + 2\xi \omega_n s + \omega_n^2} \quad (21)$$

Since the time response of the dc-voltage control loop does not need to be fast, a damping factor and a natural angular speed  $\omega_n = 2\pi \cdot 100$  rad/sec is used to obtain a critically damped response along with minimum voltage oscillation (13). The

respective integral time  $T_i=1/a$  and proportional gain  $K_p$  can be calculated as,

$$\xi = \sqrt{\frac{3}{8} \frac{k_p V_s T_i \sqrt{2}}{c_{dc} V_{dc}^*}}$$

$$\omega_n = \sqrt{\frac{3}{2} \frac{k_p V_s \sqrt{2}}{c_{dc} V_{dc}^* T_i}}$$

TABLE.I: Specified Parameters.

| Variable | Description                      | Value <sup>a</sup>        |
|----------|----------------------------------|---------------------------|
| $v_s$    | Source voltage                   | 55 [V]                    |
| $f$      | System frequency                 | 50 [Hz]                   |
| $v_{dc}$ | dc-voltage                       | 162 [V]                   |
| $C_{dc}$ | dc capacitor                     | 2200 [ $\mu F$ ] (2.0 pu) |
| $L_f$    | Filter inductor                  | 5.0 [mH] (0.5 pu)         |
| $R_f$    | Internal resistance within $L_f$ | 0.6 [ $\Omega$ ]          |
| $T_s$    | Sampling time                    | 20 [ $\mu s$ ]            |
| $T_e$    | Execution time                   | 16 [ $\mu s$ ]            |

<sup>a</sup>Note:  $V_{base} = 55$  V and  $S_{base} = 1$  kVA.

## VII SIMULATION RESULTS

A simulation model for three-phase four-leg PWM converter along with the parameters is shown in table.1 and has been developed using MATLAB-simulink. The purpose is to verify the harmonic current compensation effectiveness of the proposed control scheme under various conditions.

The proposed predictive control algorithm was involuntary using an S-function block that allows simulation of a discrete model. Simulation is performed in view of a 20 [ $\mu sec$ ] of sample time. The simulated results shown in fig. 16, the active filter starts to compensate at  $t=0.4$ . At this time, the active power filter injects an output current  $i_{ou}$  to compensate current harmonic components, current unbalanced, and neutral current.

Simultaneously. During compensation, the system currents is sinusoidal waveform as shown, with low total harmonic distortion (THD=3.93%). At  $t=0.6$ , a three-phase balanced load step change is generated from 0.6 to 1.0 p.u., which is equivalent to an 11% current imbalance. Experimental results shown in fig.10, 11, and fig.12. Which indicates the total harmonic distortion of the line current (THD<sub>i</sub>) is reduced from 9.28% to 6.71% using PI controller and the total harmonic distortion of the line current (THD<sub>i</sub>) is further reduced from 9.28% to 3.63%.

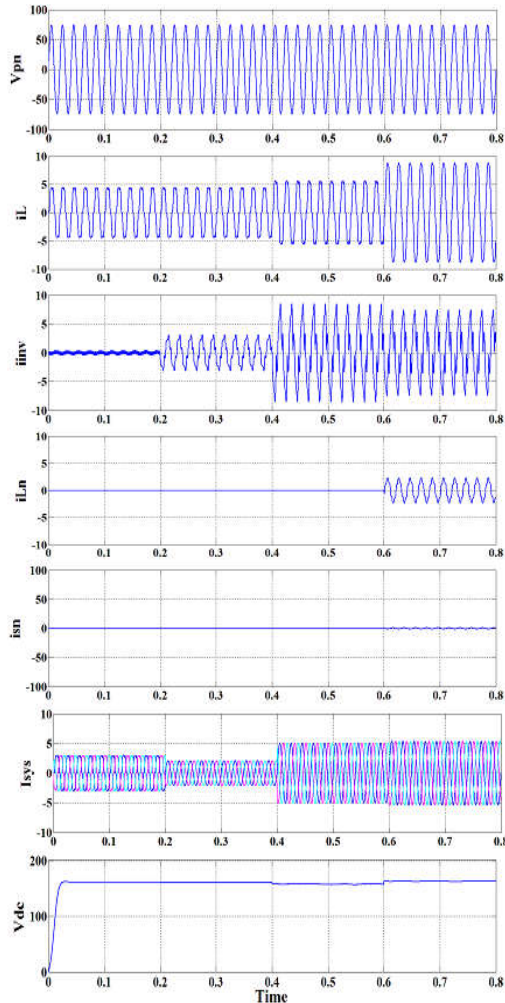


Fig. 9. Simulation results, with PI controller scheme (a) Phase to neutral source voltage. (b) Load current. (c) Active power filter output current. (d) Load neutral current. (e) System neutral current. (f) System currents. (g) DC voltage converter.

TABLE.2: Comparison of controllers.

|                      | PI  | ANFIS                   |
|----------------------|---|-------------------------|
| THD (%)              | 6.71  | 3.63                    |
| Control              | straightforward control                         | vigorous control        |
| Error Range          | Reasonable for a set of intended PI parameters. | Compensate huge errors. |
| Tuning               | physical tuning of PI parameters                | Auto tuning             |
| Membership Functions | -----   | Automatically by ANN    |

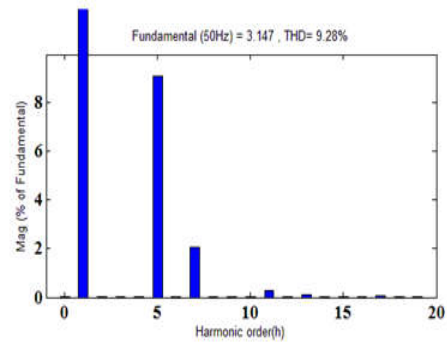


Fig.10. THD analysis of load current without any controller.

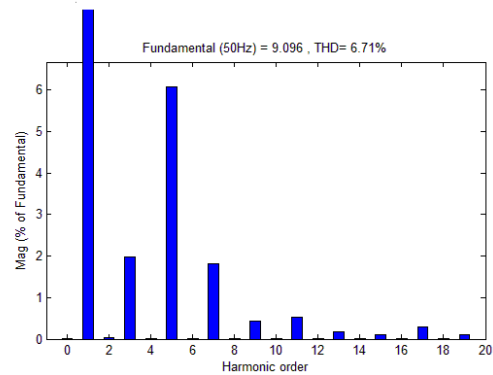


Fig.11. THD analysis of load current with PI controller.

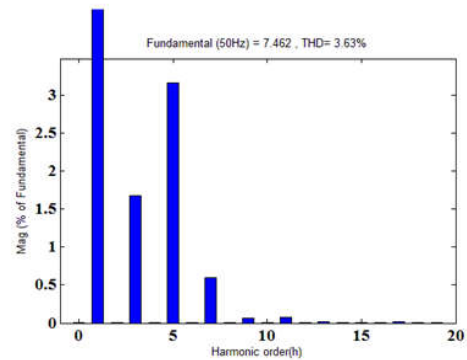


Fig.12. THD analysis of load current with ANFIS controller.

### VIII CONCLUSION

Due to the presence of non-linear loads, power quality issues will raise. The main objective of this paper is to reduce the power quality problems occurred, such as to compensate total harmonic distortion (THD), un-balanced currents generated by non-linear loads, to improve the reactive power compensation and to improve the

current tracking capability, is achieved individually results are compared. The reduction in THD as well as system currents is shown. Thus it is an effective solution to reduce power quality issues. Proposed SAPF become accustomed itself to compensate for variation in nonlinear THD percentage of source current under limits of IEEE-519 standard (5%). Simulated and experimental results have proved that the proposed predictive control algorithm is a superior alternative to classical linear control methods, in case of shunt active power filters. The predictive current control algorithm is a stable and robust solution.

## REFERENCES

- [1] Brim Singh Kamala Al-Haddad, and Ambrish Chandra, "A Review of Shunt Active Filters For Power Quality Improvement", IEEE Trans. On Industrial Electronics, Vol.46, No.5, October 1999.
- [2] N.Prabhakar and Mishra, "Dynamic Hysteresis Current Control To Minimize Switching For Three-Phase Four Leg VSI Topology To Compensate Non-Linear Load", IEEE Trans. On Power Electronics, Vol.25, No.8, Pp. 1935-1942, Aug. 2010.
- [3] P.Cortes, S.Vazquez, and L.Franquelo, "Model Predictive Control Of An Inverter With Output As LC Filter For UPS Applications", IEEE Trans. Ind. Electron., Vol.56, no.6, Pp.1875-1883, June. 2009.
- [4] J.Rodriguez, P.Correa, P.Lezzana, P.Cortes, and U.Ammann, "Predictive Current Control of A Voltage Source Inverter", IEEE Trans. Ind. Electron., Vol.54, No.1, Pp.495-503, Feb. 2007.
- [5] R.De.Aruajo Ribeiro, C.De Azevedo, and R.De Souse, "A Robust Adaptive Control Strategy Of Active Power Filters For Power Factor Correction, Harmonic Compensation And Balancing Of Non-Linear Loads", IEEE Trans. Power Electron. Vol.27, No.2, Pp.718-730, Feb. 2012.
- [6] S.Kuoro, P.Cortes, R.Vargas, U.Ammann and J.Rodriguez, "Model Predictive Control---A Simple and Powerful Method to Control Power Converters", IEEE Trans. Ind. Electron., Vol.56, No.6, Pp.1826-1838, June 2009.
- [7] D.Quevedo, R.Aguilera, M.Perez, P.Cortes and R.Lizana, "Model Predictive Control of AFE with Dynamic References", IEEE Trans. Power Electron. Vol.27, No.7, Pp.3128-3136, July. 2012.
- [8] M.Rivera, C.Rojas, B.Wu, and J.Espinoza, "Predictive Control With input filter resonance mitigation for a direct matrix converter", Vol.26, No.10, Pp.2794-2803, Oct. 2011.
- [9] P.Acuna, L.Moran, M.Riveria, J.Rodriguez, and J.Dixon, "Improved Active Filter Performance for Distribution Systems with Renewable Generation", IEEE Trans. Power Electron. Vol.27, No.9, Nov. 2012.

using two different controllers (PI/ANFIS) and the [10] Mukhtiar Singh, and Ambrish Chandra, "Real Time Implementation of ANFIS Control for Renewable Interfacing Inverter" IEEE Trans. Indus. Electronics., Vol.60.No.1. Jan. 2013.

[11] Patricio Salmeron and Jesus R. Vazquez, "Practical Design of A Three Phase Active Power Line Conditioner Controlled By Artificial Neural Networks", IEEE Trans. Power Delivery. Vol.20, No.2, April. 2005.

[12] Pramod Kumar and Alka Mahajan, "Soft Computing Techniques For The Control Active Power Filter", IEEE Trans. Power Delivery., Vol.24, No.1. Jan. 2009.

## AUTHORS PROFILE



**Mrs. K. SUVARANA** is doing M.Tech Degree in Electrical Power Systems (EPS) from Sri Krishna Devaraya University college of Engineering and Technology, Ananthapuramu 515003, A.P, India, and has graduated her B.Tech from G. Pulla Reddy Engineering College Kurnool, A.P, India., and Her areas of interest are Power Systems and Power Electronics.



**Mr. V. K. CHAKRAVARTHI NAIK** has Received his B.Tech Degree from the Sri Venkateswara University Tirupati. He received Master of Technology degree from G. Pulla Reddy Engineering College Kurnool. Currently he is working as Lecturer in the Department of Electrical and Electronics Engineering, S.K. U. College of Engineering & Technology, S.K. University, Ananthapuramu-515 003, Andhra Pradesh, India. His research area of interest are Electrical Power Systems and Reliability.

\*\*\*\*\*